

Handedness-sensitive emission of surface plasmon polaritons by elliptical nanohole ensembles

Boris B. Tsema,^{1,2} Yuri B. Tsema,¹ Maxim R. Shcherbakov,¹ Yu-Hsuan Lin,³ Da-Ren Liu,³ Vasily V. Klimov,⁴ Andrey A. Fedyanin,^{1,7} and Din Ping Tsai^{3,5,6,*}

¹Faculty of Physics, Lomonosov Moscow State University, Moscow 119991, Russia

²Moscow State Institute of Radio-engineering Electronics and Automation, Moscow 119454, Russia

³Instrument Technology Research Center, National Applied Research Laboratories, Hsinchu 30076, Taiwan

⁴Lebedev Physical Institute, Russian Academy of Sciences, Moscow, 119991 Russia

⁵Department of Physics, National Taiwan University, Taipei 10617, Taiwan

⁶Research Center for Applied Sciences, Academia Sinica, Taipei 115, Taiwan

⁷fedyanin@nanolab.phys.msu.ru

dptsai@phys.ntu.edu.tw

Abstract: We report handedness-sensitive surface plasmon polariton (SPP) emission in mirror-symmetric ensembles of elliptical nanoholes made in a thin gold film. It is found by means of rigorous calculations and scanning near-field optical microscopy that SPP excitation direction depends on the direction of circularly polarized illumination E-vector rotation. An analytical model based on anisotropic polarizability of each nanohole is presented. Both the experimental and calculated results are in agreement with Curie's principle, and contribute to better understanding of symmetry in plasmonics.

©2012 Optical Society of America

OCIS codes: (250.5403) Plasmonics; (240.6680) Surface plasmons; (180.4243) Near-field microscopy; (130.5440) Polarization-selective devices; (160.4236) Nanomaterials.

References and links

1. H. Raether, *Surface Plasmons on Smooth and Rough Surfaces and on Gratings* (Springer-Verlag, Berlin, 1988).
2. D. P. Tsai, J. Kovacs, Z. Wang, M. Moskovits, J. S. Suh, R. Botet, and V. M. Shalaev, "Photon STM images of optical excitations of fractal metal colloid clusters," *Phys. Rev. Lett.* **72**, 4149–4152 (1994).
3. H. J. Huang, C. P. Yu, H. C. Chang, K. P. Chiu, H. Ming Chen, R. S. Liu, and D. P. Tsai, "Plasmonic optical properties of a single gold nano-rod," *Opt. Express* **15**(12), 7132–7139 (2007).
4. W. T. Chen, P. C. Wu, C. J. Chen, H. Y. Chung, Y. F. Chau, C. H. Kuan, and D. P. Tsai, "Electromagnetic energy vortex associated with sub-wavelength plasmonic Taiji marks," *Opt. Express* **18**(19), 19665–19671 (2010).
5. W. T. Chen, C. J. Chen, P. C. Wu, S. Sun, L. Zhou, G. Y. Guo, C. T. Hsiao, K. Y. Yang, N. I. Zheludev, and D. P. Tsai, "Optical magnetic response in three-dimensional metamaterial of upright plasmonic meta-molecules," *Opt. Express* **19**(13), 12837–12842 (2011).
6. M. Shcherbakov, M. Dobynde, T. Dolgova, D. P. Tsai, and A. Fedyanin, "Full Poincaré sphere coverage with plasmonic nanoslit metamaterial at Fano resonance," *Phys. Rev. B* **82**(19), 193402 (2010).
7. Z. Fang, J. Cai, Z. Yan, P. Nordlander, N. J. Halas, and X. Zhu, "Removing a wedge from a metallic nanodisk reveals a fano resonance," *Nano Lett.* **11**(10), 4475–4479 (2011).
8. Z. Fang, Q. Peng, W. Song, F. Hao, J. Wang, P. Nordlander, and X. Zhu, "Plasmonic focusing in symmetry broken nanocorrals," *Nano Lett.* **11**(2), 893–897 (2011).
9. W. Chen, D. C. Abeyasinghe, R. L. Nelson, and Q. Zhan, "Experimental confirmation of miniature spiral plasmonic lens as a circular polarization analyzer," *Nano Lett.* **10**(6), 2075–2079 (2010).
10. M. R. Shcherbakov, B. B. Tsema, A. A. Ezhov, V. I. Panov, and A. A. Fedyanin, "Near-field optical polarimetry of plasmonic nanowires," *JETP Lett.* **93**(12), 720–724 (2011).
11. H. Gao, J. Henzie, and T. W. Odom, "Direct evidence for surface plasmon-mediated enhanced light transmission through metallic nanohole arrays," *Nano Lett.* **6**(9), 2104–2108 (2006).
12. S.-H. Chang, S. K. Gray, and G. C. Schatz, "Surface plasmon generation and light transmission by isolated nanoholes and arrays of nanoholes in thin metal films," *Opt. Express* **13**(8), 3150–3165 (2005).
13. R. Gordon L. K. S. Kumar, and A. G. Brolo, "Resonant light transmission through a nanohole in a metal film," *IEEE Trans. NanoTechnol.* **5**(3), 291–294 (2006).
14. S. Collin, F. Pardo, and J.-L. Pelouard, "Waveguiding in nanoscale metallic apertures," *Opt. Express* **15**(7), 4310–4320 (2007).

15. A. Degiron, H. J. Lezec, N. Yamamoto, and T. W. Ebbesen, "Optical transmission properties of a single subwavelength aperture in a real metal," *Opt. Commun.* **239**(1-3), 61–66 (2004).
 16. K. L. van der Molen, K. J. Klein Koerkamp, S. Enoch, F. B. Segerink, N. F. van Hulst, and L. Kuipers, "Role of shape and localized resonances in extraordinary transmission through periodic arrays of subwavelength holes: Experiment and theory," *Phys. Rev. B* **72**(4), 045421 (2005).
 17. J. Jin, *The Finite-Element Method in Electromagnetics* (Wiley, New York, 1993).
 18. J. D. Jackson, *Classical Electrodynamics*, 3rd Ed. (Wiley, New York, 1998).
 19. E. Hartmann, *An Introduction to Crystal Physics* (University College Cardiff Press, Cardiff, Wales, 1984).
-

1. Introduction

Surface plasmon-polaritons (SPPs) are two-dimensional waves bound to metal-dielectric interface [1] capable of optical energy localization and transfer at unprecedentedly low scales [2–5] as well as creation of highly-efficient polarization-sensitive metasurfaces [6]. In order to be able to address plasmonic signal correctly, it is important to have an ability of controlling the direction of SPP emission. For this purpose one can use different degrees of freedom of light, which excites SPP, and, particularly, its polarization state. It was shown that plasmonic emission direction and/or amplitude could be controlled by polarization at flat metal surfaces, protrusions and apertures of different shapes [7–9], as well as at isolated plasmonic objects [10]. In previous works the important role of symmetry of the plasmon-emitting structures and its connection to light polarization was pointed out. Although, handedness-sensitive—i.e. sensitive to whether impinging light is right-hand or left-hand circularly polarized—SPP launching was only observed in structures possessing planar chirality [9]. In this paper we present a novel 3λ -sized nanohole-based quasi-planar device which, even though possessing mirror symmetry, is a source of handedness-sensitive SPPs. The results are obtained numerically, experimentally and analytically. The observed effect rises from interference between SPPs launched from different point-like sources and is perfectly following the Curie's symmetry principle.

2. Sample design and fabrication

For handedness-sensitive emission of SPPs, an ensemble of elliptical nanoholes perforated in a thin gold film is considered. The samples under study comprise three elliptical nanoholes in the corners of an equilateral triangle. The major axis of the ellipse pointing to the center of the triangle as depicted in Fig. 1(a).

A single nanohole illuminated by a linearly polarized plane wave from one side of the film is capable of becoming a source of SPPs on the other side of the film. The mean SPP propagation direction coincides with the direction of the illuminating wave E -vector [11,12]. Additionally, the amplitude of the SPP launched this way is proportional to overall transmission efficiency of the nanohole at the polarization and wavelength being used. In case of elliptical subwavelength nanoholes the transmission coefficient is larger for light polarized along the *minor* ellipse axis than for one polarized along the major one due to extended cutoff wavelength of such a waveguide [13, 14]. The spectrum of such a nanohole contains a shape resonance which was proved analytically [13] and experimentally [15, 16]. At this wavelength the nanohole is an efficient source of SPPs for light polarized along the minor axis of the ellipse and faintly emits SPPs for light polarized along the major axis.

Described ensemble of three nanoholes acts like a triple SPP source where each of the sources is a point-like polarization-sensitive SPP emitter. If the ensemble is illuminated by a circularly polarized plane wave the ellipses emit SPP with different phase shift because the effective SPP emission takes place only when E -field is perpendicular to the ellipse's major axis. In other words, ellipses turn on and off in a consequence. The direction of the consequence coincides with that of the circularly polarized wave E -field rotation direction. The phase delay between the sources is defined by handedness of the illumination and governs the interference pattern of surface plasmons.

For experimental observation of handedness-sensitive SPP emission a set of nanohole ensembles were fabricated by means of focused ion-beam (FIB) lithography on a 80-nm-thick thermally sputtered golden film on a glass substrate. FEI Nova 200 dual beam system with

fabrication resolution about 30 nm was used. Major axis of the holes b and the distance from the holes to the center of ensemble d was varied. 20 samples were fabricated with designed hole-to-center distance values of $d = 50$ nm, 100 nm, 200 nm, 300 nm and 500 nm, and major axis length values of $b = 200$ nm, 300 nm, 400 nm and 500 nm. The actual dimensions of the sample underwent severe deviations from the dimensions of the design file. Figure 1(a) shows a scanning electron microscope image of a typical sample with actual dimensions $a = 100$ nm, $b = 300$ nm, $d = 250$ nm. The imperfections of the shape and dimensions of the apertures are a result of high thickness of the film subject to FIB lithography and the polycrystalline structure of the film.

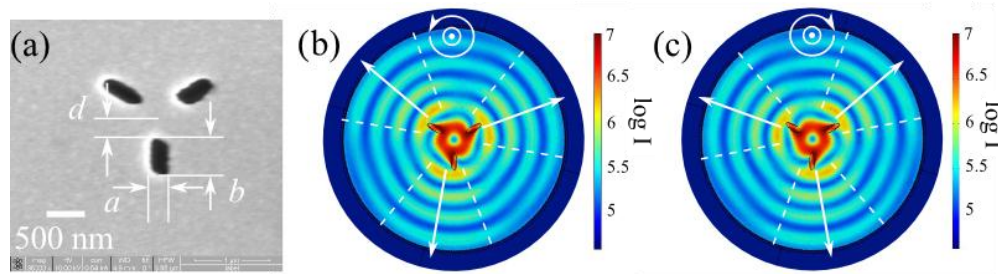


Fig. 1. a) A scanning electron micrograph of an elliptical nanohole ensemble sample milled in a gold film by focused ion beam. The dimensions notation is as follows: a stands for minor ellipse axis length, b is for major ellipse axis length, d is for distance between the inner edges of the ellipses and the center of the ensemble and t is for the thickness of the film. b)-c) Finite element simulations of the logarithmic-scale electromagnetic field intensity at a subwavelength height from the elliptical nanohole ensemble with $a = 100$ nm, $b = 300$ nm, $d = 250$ nm and $t = 150$ nm illuminated by left-hand (b) and right-hand (c) circularly polarized light at $\lambda = 820$ nm. Handedness-sensitive emission of SPPs, which direction and boundaries are marked with arrows and dashed lines, respectively, is observed.

3. Numerical simulation results

Handedness-sensitive SPP emission was verified by finite element method rigorous calculations (COMSOL Multiphysics v4 RF Module, Electromagnetic Waves interface) as shown in Figs. 1(b), 1(c). Computational cell was chosen to be a cylinder with 2 μm radius, 300 nm height and perfectly matched layer (PML) as boundary conditions from all sides of the cell. The PML was defined as a generic type PML with the thickness of a wavelength being used. It was covered with scattering boundaries from outside and the swept meshing technique was chosen with the direction from inner to outer boundaries of PML with the 5-layer distribution. Such definition of the boundary conditions excluded spurious reflections back to the computational cell. Delaunay meshing technique was used to avoid cell shape reflection in the mesh of the film boundaries. The structure was excited by a monochromatic circularly polarized plane wave analytically defined in the whole computational volume; the wavelength $\lambda = 820$ nm was chosen to match the approximate position of the shape resonance of individual nanoholes, which was estimated using known expressions [13,14]. The problem was solved for the scattered evanescent fields which rise from the presence of golden scatterers [17] at the distance of 10 nm from the sample surface. Figures 1(b) and 1(c) show the electromagnetic field intensity at this distance from the elliptical nanohole ensemble with $a = 100$ nm, $b = 300$ nm, $d = 250$ nm and a film thickness of 150 nm illuminated by the left-hand and right-hand circularly polarized light, respectively. Emission of SPPs is observed at different angles for different incident light polarizations, which is denoted with arrows and dashed lines for the sake of clarity. Thus, the evidence of handedness-sensitive SPP emission is provided.

4. Scanning near-field optical microscopy results

A schematic of the scanning near-field optical microscopy (SNOM) setup used to study handedness-sensitive SPP emission in elliptical nanohole ensembles experimentally is shown

in Fig. 2. A commercial Veeco Aurora-3 transmission collection-mode SNOM with tapered optical fiber tip was used. Tip produced by Veeco with an average aperture of 50-80 nm was placed at 10 nm-vicinity of the sample by a feedback-looped sample piezo-stage.

The sample was illuminated by chopped CW light with 10 mW of average optical power before the chopper at the wavelength $\lambda = 647$ nm (Coherent Innova 70C-Spectrum) focused by an objective lens with NA = 0.65 to the laser beam spot with the diameter of 50 μm . The wavelength was chosen from all the wavelengths available from the source to be as close to the shape resonance of the nanoholes as possible. Ellipticity of the incident wave polarization state was measured by a thin-film polarizer to be approximately 90% in the sample plane; the imperfection of the polarization state is explained by the silver mirror used to deflect the beam to the site of the microscope objective. Optical signal was collected by a photomultiplier tube (PMT) and passed through a low-noise preamplifier to a lock-in amplifier. The magnitude signal from the lock-in amplifier was used as an input to the SNOM controller.

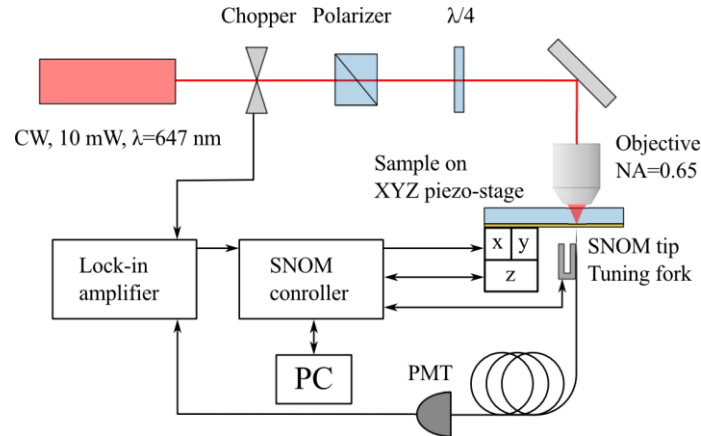


Fig. 2. A SNOM setup for experimental observation of handedness-sensitive SPP emission

Figure 3 shows optical near-field signal as measured with the SNOM in the vicinity of a nanohole ensemble sample with left-handed and right-handed circularly polarized backside illumination. The sample with the following dimensions was studied: $a = 100$ nm, $b = 500$ nm, $d = 250$ nm. Other samples did not give satisfactory results which is discussed in Sec. 6. Several visually determined SPP propagation directions are observed in Figs. 3(b), 3(c). The directions marked with the solid arrows denote ones that depend on the handedness of the used illumination. Intensity of SPPs is switched from one direction to another by changing the impinging light polarization from left-hand circularly polarized to right-hand circularly polarized. There are also several directions which appear in both right- and left-hand circularly polarized illumination; these are marked with the dashed arrows.

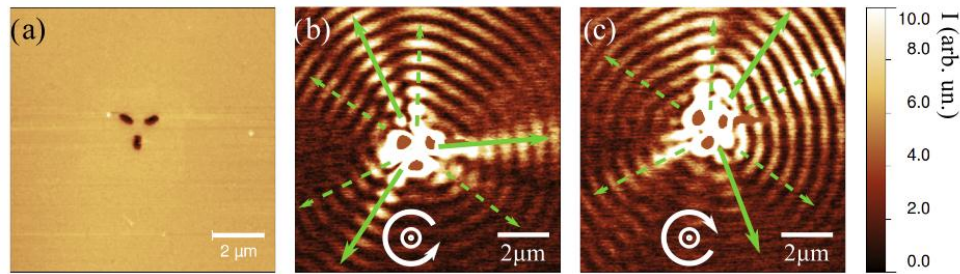


Fig. 3. a) A shear-force topography image of an elliptical nanohole ensemble sample. As extracted from scanning electron microscopy sample dimensions are: $a = 100$ nm, $b = 500$ nm, $d = 250$ nm. b), c) SNOM images of the sample taken with backside left-hand and right-hand circularly polarized light illumination, respectively. SPP waves considered as handedness sensitive ones are marked with solid arrows. The dashed arrows denote the SPP directions either present for both polarizations either rising from the imperfection of the sample.

5. Analytical model for handedness-sensitive electromagnetic response of an ensemble of dipoles

In this section we provide a proof of the handedness-sensitive electromagnetic response of the nanoholes by considering them as three anisotropic dipoles \mathbf{d}_i , $i = 1, 2, 3$ with polarizability only along their respective axes, that is the polarizability tensor for i -th dipole will have the form:

$$\alpha_{kl}^{(i)} = \xi V n_k^{(i)} n_l^{(i)}, \quad (1)$$

where $\mathbf{n}^{(i)}$, $i = 1, 2, 3$ are unit vectors from the center of the dipole ensemble to the i -th dipole, k and l denote Cartesian coordinates, V is the nanohole volume and ξ is a dimensionless parameter which depends on the hole shape, material of the of film and illumination wavelength. To have a very rough idea about the dependence of ξ on these parameters, one can approximate the holes by spheroids with c as a long semiaxis and a as a short semiaxis. In this case we have

$$\xi = \frac{1}{4\pi} \frac{(\varepsilon(\omega) - 1)(1 - \bar{\varepsilon})}{(\varepsilon(\omega) - \bar{\varepsilon})}, \quad \bar{\varepsilon} = \frac{\xi_0(-2\xi_0 + (\xi_0^2 - 1)\ln((\xi_0 + 1)/(\xi_0 - 1)))}{(\xi_0^2 - 1)(-2 + \xi_0 \ln((\xi_0 + 1)/(\xi_0 - 1)))} \quad (2)$$

where $\varepsilon(\omega) = \varepsilon_{\text{hole}} / \varepsilon_{\text{metal}}(\omega)$ is relative permittivity of holes and $\xi_0 = c / \sqrt{c^2 - a^2}$ is a geometric parameter.

If one assumes that all dipoles are in plane $z = 0$, the coordinates of their centers are:

$$\begin{aligned} \mathbf{r}^{(1)} &= h[0, 1, 0]; \\ \mathbf{r}^{(2)} &= h[\sqrt{3}/2, -0.5, 0]; \\ \mathbf{r}^{(3)} &= h[-\sqrt{3}/2, -0.5, 0], \end{aligned} \quad (3)$$

where $h = d + b/2$. To describe the interaction between the dipoles and external field \mathbf{E}_0 , we use retarded Green function $\hat{G}_0(\mathbf{r}, \mathbf{r}', \omega)$ in free space, which is the solution of Maxwell equation:

$$\nabla \times (\nabla \times \hat{G}_0(\mathbf{r}, \mathbf{r}', \omega)) - \left(\frac{\omega}{c}\right)^2 \hat{G}_0(\mathbf{r}, \mathbf{r}', \omega) = 4\pi \left(\frac{\omega}{c}\right)^2 \hat{1} \delta(\mathbf{r} - \mathbf{r}'), \quad (4)$$

and has the following form [18]:

$$G_{0,i,j}(\mathbf{r}, \mathbf{r}', \omega) = \left[(\delta_{ij} - n_i n_j) + \frac{3n_i n_j - \delta_{ij}}{k^2} \left(\frac{1}{|\mathbf{r} - \mathbf{r}'|^2} - \frac{ik}{|\mathbf{r} - \mathbf{r}'|} \right) \right] \frac{e^{ik|\mathbf{r} - \mathbf{r}'|}}{|\mathbf{r} - \mathbf{r}'|}, \quad (5)$$

where $\mathbf{n} = (\mathbf{r} - \mathbf{r}')/|\mathbf{r} - \mathbf{r}'|$ is a unit vector directed from the point \mathbf{r} to \mathbf{r}' . Now the dipole momenta of all nanoholes can be found by solving the following system of linear equations:

$$\begin{aligned} \mathbf{d}_1 &= \hat{\alpha}_1 (\mathbf{E}_0 + \hat{G}_0(\mathbf{r}_1 - \mathbf{r}_2, \omega) \mathbf{d}_2 + \hat{G}_0(\mathbf{r}_1 - \mathbf{r}_3, \omega) \mathbf{d}_3); \\ \mathbf{d}_2 &= \hat{\alpha}_2 (\mathbf{E}_0 + \hat{G}_0(\mathbf{r}_2 - \mathbf{r}_1, \omega) \mathbf{d}_1 + \hat{G}_0(\mathbf{r}_2 - \mathbf{r}_3, \omega) \mathbf{d}_3); \\ \mathbf{d}_3 &= \hat{\alpha}_3 (\mathbf{E}_0 + \hat{G}_0(\mathbf{r}_3 - \mathbf{r}_1, \omega) \mathbf{d}_1 + \hat{G}_0(\mathbf{r}_3 - \mathbf{r}_2, \omega) \mathbf{d}_2). \end{aligned} \quad (6)$$

In these equations the terms with retarded Green functions describe the dipole interactions between the holes. Multiplying these equations by $\mathbf{n}^{(i)}$ and making use of Eq. (1) one can obtain:

$$\begin{aligned}
d_1 &= \xi V \left(n^{(1)} E_0 + n^{(1)} \hat{G}_0(r_1 - r_2, \omega) n^{(2)} d_2 + n^{(1)} \hat{G}_0(r_1 - r_3, \omega) n^{(3)} d_3 \right); \\
d_2 &= \xi V \left(n^{(2)} E_0 + n^{(2)} \hat{G}_0(r_2 - r_1, \omega) n^{(1)} d_1 + n^{(2)} \hat{G}_0(r_2 - r_3, \omega) n^{(3)} d_3 \right); \\
d_3 &= \xi V \left(n^{(3)} E_0 + n^{(3)} \hat{G}_0(r_3 - r_2, \omega) n^{(2)} d_2 + n^{(3)} \hat{G}_0(r_3 - r_1, \omega) n^{(1)} d_1 \right).
\end{aligned} \quad (7)$$

where d_i are the amplitudes of the dipoles, $\mathbf{d}_i = d_i \mathbf{n}^{(i)}$.

Due to the system symmetry the following restrictions apply:

$$\begin{aligned}
\mathbf{n}^{(1)} \hat{G}_0(\mathbf{r}_1 - \mathbf{r}_2, \omega) \mathbf{n}^{(2)} &= \mathbf{n}^{(1)} \hat{G}_0(\mathbf{r}_1 - \mathbf{r}_3, \omega) \mathbf{n}^{(3)} = \mathbf{n}^{(2)} \hat{G}_0(\mathbf{r}_2 - \mathbf{r}_3, \omega) \mathbf{n}^{(3)} = c; \\
d_1 + d_2 + d_3 &= 0.
\end{aligned} \quad (8)$$

Finally, the solution is obtained:

$$d_i = \frac{\xi V}{1 + c \xi V} \mathbf{n}^{(i)} \mathbf{E}_0. \quad (9)$$

The total electric field from all the dipoles and the external field is expressed as follows:

$$E(\mathbf{r}) = E_0 + \frac{1}{1 + c \xi V} \left(\hat{G}_0(\mathbf{r} - \mathbf{r}_1, \omega) \hat{\alpha}_1 + \hat{G}_0(\mathbf{r} - \mathbf{r}_2, \omega) \hat{\alpha}_2 + \hat{G}_0(\mathbf{r} - \mathbf{r}_3, \omega) \hat{\alpha}_3 \right) E_0 \quad (10)$$

Total electric field intensities for incident left-hand $\mathbf{E}_0 = [1, -i, 0] \exp(ikz)$ and right-hand $\mathbf{E}_0 = [1, i, 0] \exp(ikz)$ circularly polarized waves was calculated; their difference is shown in Fig. 4 for $2\pi h/\lambda = 1$ as a function of x and y . It is seen that intensities of the electric field for right- and left-hand circular polarizations are different and handedness-sensitive pattern on the E-field intensity is present in this system. From mathematical point of view, it results from tensorial and complex nature of Green functions in Eq. (10). It is important to mention that the absolute value of the intensity difference reaches its maximum value for $2\pi h/\lambda \sim 1$. For $2\pi h/\lambda \ll 1$ the planar distribution is similar to shown in Fig. 4 but its absolute value is $(kh)^3$ times less. It is due to the fact that for small systems the fields could be considered quasistatic with the same phase for every point of the system. On the other hand, for $2\pi h/\lambda \gg 1$ the interaction between holes becomes small. Thus, the model provides the qualitative description of the handedness-sensitive electromagnetic response of mirror-symmetric dipole ensembles.

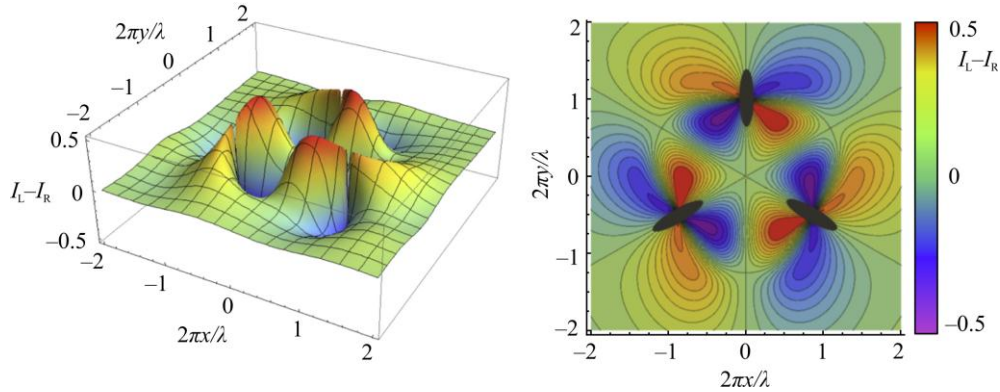


Fig. 4. The distribution of difference of intensities for right- and left-hand circularly polarized illumination in plane of holes ($z = 0$) under $2\pi h/\lambda = 1$ condition. Black ellipses denote the nanoholes position.

6. Discussion: Curie's principle for surface plasmons

Numerical, experimental and analytical results indicate the mirror symmetry breaking in the optical near-field by surface plasmons. This is in perfect agreement with Curie's symmetry

principle which states that a medium under an external influence exhibits only those symmetry elements that are common to the medium without the influence and the influence without the medium [19]. Since the perfect nanohole ensemble belongs to $p3m$ planar symmetry group and circularly polarized light could be associated with $p\infty$ symmetry, the resulting electromagnetic field distribution is of $p3$ symmetry.

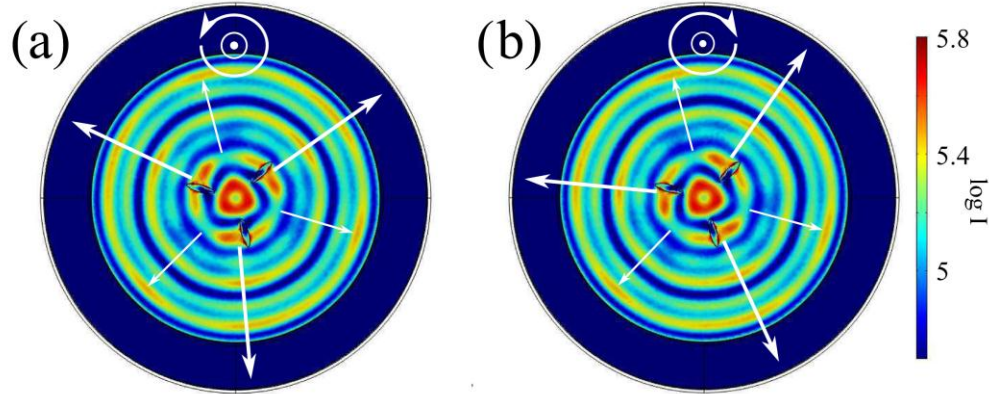


Fig. 5. Finite element simulations of the elliptical nanohole ensemble with $a = 100$ nm, $b = 500$ nm and $d = 250$ nm illuminated by the left-hand (a) and right-hand (b) circularly polarized light at $\lambda = 650$ nm which corresponds to experimental situation. Large arrows indicate SPP waves, which are switched with illumination polarization change, and small arrows indicate ones that do not.

As it could be seen from SNOM measurements the effect is very sensitive to the sample quality and dimensions. Only one of 20 fabricated nanohole ensembles with different a , b and d values was able to give pronounced evidence of handedness-sensitive SPP emission. Illumination wavelength is also crucial. It is seen in Fig. 5 by means of finite element calculations that effect is less pronounced in the experimentally studied sample than in the initially supposed one because one does not excite the shape resonance effectively using the wavelength $\lambda = 647$ nm. The performance of the device could be optimized by picking the proper size of the apertures, which governs the shape resonance position, and distance between them, which governs the interference of SPPs at a fixed wavelength. The provided data and the model are believed to confirm that mirror-symmetric plasmonic nanostructures are capable of handedness-sensitive SPP emission.

7. Conclusions

Handedness-sensitive surface plasmon polariton emission from mirror-symmetric elliptical nanohole ensembles was observed. It was shown using scanning near-field optical microscopy and numerical calculations that direction of surface plasmons launched by the sample could be switched by changing illumination polarization from left- to right-hand circularly polarized. The established effect is supported by an analytical model and could find practical applications in new plasmonic circuitry devices.

Acknowledgments

The authors would like to acknowledge Russian Foundation for Basic Research (RFBR) support (grant 11-02-92009) and the assistance of Anton Le. Authors also thank financial aids from National Science Council, Taiwan under grant numbers 99-2911-I-002-127, 99-2120-M-002-012, 100-2923-M-002-007-MY3 and 100-2120-M-002-008. Authors are grateful to National Center for Theoretical Sciences, Taipei Office, Molecular Imaging Center of National Taiwan University and National Center for High-Performance Computing, Taiwan for their support. V. Klimov would like to express his gratitude to the RFBR (grants ## 11-02-91065, 11-02-92002, 11-02-01272, 12-02-90014) for financial support.